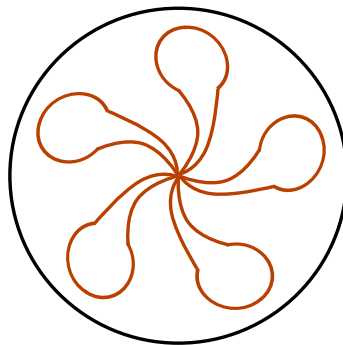




Faculty of Engineering, Computer and Mathematical Sciences  
School of Mechanical Engineering

# The Emissions and Chemical Autoignition Delay of Biodiesel Fuel



*Author*

Marcus Boyd

*Supervisors*

Assoc. Prof. Con Doolan

Assoc. Prof. Colin Kestell

22 February 2013



# Contents

<b>List of Figures</b>	<b>iv</b>
<b>List of Tables</b>	<b>viii</b>
<b>Abstract</b>	<b>ix</b>
<b>Nomenclature</b>	<b>xiii</b>
<b>1 Introduction</b>	<b>1</b>
1.1 Background . . . . .	1
1.2 Aims and objectives . . . . .	1
1.3 Contribution to the field . . . . .	3
1.4 Structure of this document . . . . .	4
<b>2 Background</b>	<b>7</b>
2.1 Biodiesel and its properties . . . . .	7
2.2 Compression ignition combustion . . . . .	14
2.2.1 Apparent heat release rate . . . . .	14
2.2.2 Spray combustion . . . . .	15
2.2.3 Ignition delay . . . . .	20
2.2.3.1 Cetane test . . . . .	23
2.2.3.2 Arrhenius reaction rate . . . . .	23
2.2.3.3 Elementary reactions . . . . .	25
2.2.3.4 Autoignition chemical kinetics . . . . .	26
2.3 Emissions . . . . .	28
2.3.1 Nitrogen oxides . . . . .	30
2.3.1.1 Formation mechanisms . . . . .	30
2.3.2 Particulate matter . . . . .	32
2.3.3 Unburnt hydrocarbons . . . . .	34
2.4 Simulation of compression ignition combustion . . . . .	34
2.4.1 Sub-models . . . . .	37
2.4.1.1 KH-RT hybrid droplet breakup model . . . . .	38
2.4.1.2 Multicomponent droplet evaporation . . . . .	39
2.4.1.3 Emissions formation . . . . .	39
2.4.2 Shell autoignition model . . . . .	40
2.4.2.1 Chemical background . . . . .	40
2.4.2.2 Shell model mechanism . . . . .	41

2.4.3	Detailed chemical kinetic mechanisms . . . . .	45
2.5	Techniques for investigating chemical autoignition delay . . . . .	49
2.5.1	Constant volume chamber . . . . .	49
2.5.2	Rapid compression machine . . . . .	50
2.5.3	Flow reactor . . . . .	51
2.5.4	Visualised engine . . . . .	51
2.5.5	Shock tube . . . . .	54
2.5.5.1	Operating principles . . . . .	55
2.5.5.2	Potential errors . . . . .	60
2.6	Conclusion . . . . .	62
<b>3</b>	<b>Literature review</b>	<b>65</b>
3.1	Current research into formation of nitrogen oxides . . . . .	65
3.2	3-D biodiesel simulations . . . . .	71
3.2.1	Ignition delay modelling . . . . .	72
3.3	Chemical autoignition delay experiments . . . . .	73
3.3.1	Relevant fuels . . . . .	74
3.3.2	Published results . . . . .	74
3.4	Aerosol shock tube . . . . .	81
3.5	Conclusion . . . . .	87
3.5.1	Gap statement . . . . .	88
<b>4</b>	<b>Engine experiment method</b>	<b>89</b>
4.1	Apparatus . . . . .	89
4.1.1	Performance measurement . . . . .	91
4.1.2	Emissions measurement . . . . .	93
4.1.3	Apparent heat release rate . . . . .	96
4.2	Experimental method . . . . .	96
4.3	Data processing . . . . .	97
4.4	Summary . . . . .	102
<b>5</b>	<b>Engine experiment results</b>	<b>103</b>
5.1	Fuel analysis . . . . .	104
5.2	Apparent heat release rates . . . . .	106
5.3	Emissions and the timing of injection and combustion . . . . .	118
5.3.1	Error analysis . . . . .	118
5.3.2	Results . . . . .	120
5.4	Wall impingement hypothesis . . . . .	132
5.5	Conclusion . . . . .	133
<b>6</b>	<b>Shock tube experimental design and method</b>	<b>135</b>
6.1	Required experimental conditions . . . . .	135
6.2	Sizing . . . . .	136
6.2.1	Theory . . . . .	136
6.2.2	Diameter . . . . .	138
6.2.3	Length . . . . .	139
6.2.4	L1d simulations . . . . .	141

6.2.4.1	Governing equations . . . . .	142
6.2.4.2	Results . . . . .	143
6.3	Mechanical design . . . . .	148
6.3.1	Diaphragm . . . . .	148
6.3.2	Test section . . . . .	149
6.4	Fuel evaporation . . . . .	155
6.4.1	Pre-evaporated method . . . . .	155
6.4.2	Single drop method . . . . .	156
6.5	Instrumentation . . . . .	158
6.5.1	Optical system . . . . .	161
6.5.2	Data processing . . . . .	161
6.5.2.1	Filtering . . . . .	162
6.5.2.2	Shock speed measurement . . . . .	166
6.5.2.3	Ignition delay . . . . .	169
6.6	Pressure testing . . . . .	179
6.7	Operation method . . . . .	179
6.8	Summary . . . . .	180
<b>7</b>	<b>Shock tube results</b>	<b>181</b>
7.1	Preliminary work . . . . .	182
7.1.1	Fuel loading . . . . .	182
7.1.2	Validation with <i>n</i> -dodecane . . . . .	182
7.1.3	Temperature correction . . . . .	187
7.2	Diesel . . . . .	194
7.3	Methyl oleate . . . . .	197
7.4	Discussion . . . . .	199
7.4.1	Large negative temperature coefficient region . . . . .	199
7.4.2	High temperature results . . . . .	200
7.5	Fuel comparison . . . . .	201
7.6	Conclusion . . . . .	203
<b>8</b>	<b>Conclusion</b>	<b>205</b>
8.1	Engine experiment . . . . .	205
8.2	Shock tube . . . . .	206
8.3	Engine and shock tube ignition delay . . . . .	206
8.4	Future work . . . . .	210
<b>Appendix A Introduction to compression ignition engines</b>		<b>213</b>
A.1	Combustion conditions . . . . .	215
A.2	Fuel injection . . . . .	216
<b>Appendix B Derivation of apparent heat release rate</b>		<b>221</b>
<b>Appendix C Fuel data</b>		<b>225</b>
<b>Appendix D Chemical ignition delay measurements</b>		<b>235</b>
<b>Bibliography</b>		<b>239</b>

# List of Figures

1.1	The permanent haze over Sha Tin Racecourse in Hong Kong . . . .	2
2.1	Oleic acid methyl ester . . . . .	10
2.2	A triglyceride molecule . . . . .	11
2.3	The biodiesel transesterification reaction . . . . .	12
2.4	The biodiesel transesterification reaction with ethanol . . . . .	13
2.5	Typical heat release rate plot . . . . .	15
2.6	Direct injection combustion conceptual model . . . . .	17
2.7	Conceptual model apparent heat release rate . . . . .	18
2.8	Direct injection combustion conceptual model for mixing controlled combustion . . . . .	19
2.9	Illustration of the typical effect of ignition delay on the heat release rate . . . . .	20
2.10	Heat release rate vs. crank angle, showing maximum, and the maximum of first and second differentials . . . . .	21
2.11	Chemical autoignition delay compared to total ignition delay . . . .	22
2.12	Shock tube ignition delay data demonstrating negative temperature coefficient behaviour . . . . .	27
2.13	Smoke vs. oxygen content . . . . .	34
2.14	Chemicals modelled by detailed mechanisms . . . . .	47
2.15	Reaction path diagram for hydrocarbon ignition . . . . .	48
2.16	Rapid compression machine . . . . .	50
2.17	Flow reactor . . . . .	52
2.18	Visualised engine . . . . .	54
2.19	Basic shock tube . . . . .	55
2.20	Time vs. position for the formation of a shock wave from piston movement . . . . .	56
2.21	Flow with reference frame attached to the shock front . . . . .	57
2.22	Time vs. position for the formation of a rarefaction wave from piston movement . . . . .	58
2.23	Shock tube zones . . . . .	59
2.24	Effect of shock tube diameter on test temperature stability . . . . .	61
3.1	Emissions of nitrogen oxides as a function of timing of the maximum cylinder temperature for high load . . . . .	66
3.2	Emissions of nitrogen oxides as a function of the timing of maximum cylinder temperature for low load . . . . .	67

3.3	Correlation of $EI_{NO_x}$ normalised by $EI_{NO_x}$ at standard conditions with reciprocal of stoichiometric flame temperature for <i>direct injection engines</i> . . . . .	69
3.4	Correlation of $EI_{NO_x}$ normalised by $EI_{NO_x}$ at standard conditions with reciprocal of stoichiometric flame temperature for <i>indirect injection engines</i> . . . . .	70
3.5	Data used to adapt the Shell model to diesel . . . . .	73
3.6	1-Methylnaphthalene . . . . .	74
3.7	Diesel surrogate ignition delay data from the literature . . . . .	78
3.8	The driver section of the Stanford Aerosol Shock Tube . . . . .	82
3.9	Operation procedure of an aerosol shock tube . . . . .	83
3.10	A view of the Stanford Aerosol Shock Tube looking down the tube from the optical table . . . . .	85
3.11	Evaporation time vs. temperature behind the incident shock wave for an aerosol of approximately $5\ \mu\text{m}$ . . . . .	86
3.12	Diffusion relaxation time vs. fuel loading for different droplet sizes . . . . .	86
3.13	Measurements of <i>n</i> -dodecane ignition delay in an aerosol shock tube compared to heated shock tube measurements . . . . .	87
4.1	Experimental schematic . . . . .	90
4.2	Dynamometer . . . . .	92
4.3	Fuel measurement system . . . . .	93
4.4	Sampling port in exhaust coupling . . . . .	94
4.5	Venturi meter cross section . . . . .	95
4.6	Pressure transducer locations . . . . .	97
4.7	Data processing program flowchart . . . . .	98
4.8	Different designs of the Savitzky–Golay filter . . . . .	99
4.9	Experimental conditions for 80% tallow/20% canola oil biodiesel — case 5 . . . . .	100
4.10	Ideal heat release rate with derivatives . . . . .	101
5.1	Gas chromatography and mass spectrometry results — ester profile . . . . .	105
5.2	Apparent heat release rate for #2 diesel at different loads . . . . .	107
5.3	Apparent heat release rate for 100% tallow biodiesel at all loads . . . . .	108
5.4	Apparent heat release rate for 50% tallow/50% palm oil biodiesel at all loads . . . . .	109
5.5	Apparent heat release rate for methyl tallowate at all loads . . . . .	111
5.6	Apparent heat release rate for 80% tallow/20% canola oil biodiesel at all loads . . . . .	112
5.7	Apparent heat release rate at approximately 50% load for all fuels . . . . .	114
5.8	Apparent heat release rate at approximately 80% load for all fuels . . . . .	116
5.9	Apparent heat release rate at approximately 93% load for all fuels . . . . .	117
5.10	Specific particulate matter vs. output . . . . .	120
5.11	Specific particulate matter vs. output, comparing #2 diesel to biodiesel . . . . .	121
5.12	Specific emissions of nitrogen oxides vs. output . . . . .	122
5.13	Start of injection vs. output . . . . .	124
5.14	Ignition delay vs. output . . . . .	125

5.15	Fuel consumption vs. output . . . . .	126
5.16	Specific nitrogen oxides vs. ignition delay . . . . .	128
5.17	Specific nitrogen oxides vs. start of combustion . . . . .	129
5.18	Particulate matter vs. ignition delay . . . . .	130
6.1	$x-t$ diagram showing zone numbers for a reflected shock tube . . . . .	137
6.2	$x-t$ diagram with helium driver and test conditions of 25 bar and 800 K . . . . .	140
6.3	$x-t$ diagram with test conditions of 25 bar and 800 K and a driver extension . . . . .	141
6.4	L1d control-mass cell . . . . .	142
6.5	$x-t$ diagram of the University of Adelaide Shock Tube design with an air driver generating 800 K test conditions . . . . .	144
6.6	Fuel position, pressure and temperature history with air driver generating 800 K test conditions . . . . .	144
6.7	$x-t$ diagram of the University of Adelaide Shock Tube design with an air driver generating 1300 K test conditions . . . . .	145
6.8	Fuel position, pressure and temperature history with air driver generating 1300 K test conditions . . . . .	145
6.9	$x-t$ diagram of the University of Adelaide Shock Tube design with a helium driver generating 20 bar and 1200 K test conditions . . . . .	146
6.10	Fuel position, pressure and temperature history for a helium driver generating 20 bar and 1200 K test conditions . . . . .	146
6.11	$x-t$ diagram of the University of Adelaide Shock Tube design with a helium driver generating 20 bar and 800 K test conditions . . . . .	147
6.12	Fuel position, pressure and temperature history for a helium driver generating 20 bar and 800 K test conditions . . . . .	147
6.13	The University of Adelaide Shock Tube before fitting gas lines . . . . .	148
6.14	Cross section of the diaphragm clamping mechanism . . . . .	150
6.15	Cross section of the test section . . . . .	151
6.16	Exploded view of the test section . . . . .	153
6.17	10 $\mu$ L drop suspended from wire . . . . .	154
6.18	Deformed wire after experiment . . . . .	154
6.19	Test section undergoing hydrostatic pressure testing . . . . .	155
6.20	Single drop method . . . . .	157
6.21	$n$ -Dodecane experimental evaporation times in the Stanford Aerosol Shock Tube . . . . .	157
6.22	Test section instrumentation schematic . . . . .	160
6.23	Unfiltered and filtered pressure measurements . . . . .	163
6.24	Photomultiplier signal from an incandescent light source . . . . .	164
6.25	Photomultiplier signal characterisation . . . . .	165
6.26	Cross-correlation technique . . . . .	167
6.27	Cross-correlation technique and weighting function with endwall data	168
6.28	Close up of cross-correlation technique and weighting function with sidewall data . . . . .	169
6.29	$x-t$ diagram of the start of ignition . . . . .	170
6.30	Definition of chemiluminescence signal characteristic times . . . . .	171

6.31	Simulated CH* emission . . . . .	172
6.32	Ignition signals . . . . .	173
6.33	Ignition signals at low temperature . . . . .	174
6.34	Ignition signals at high temperature . . . . .	175
6.35	Superimposed ignition signals hypothesis illustration . . . . .	177
6.36	$x-t$ diagram of ignition hypothesis . . . . .	178
6.37	Comparing ignition delay measurement methods . . . . .	178
7.1	8 $\mu\text{L}$ compared to 4 $\mu\text{L}$ results . . . . .	183
7.2	$n$ -Dodecane ignition delay data from the literature . . . . .	184
7.3	$n$ -Dodecane ignition delay comparison . . . . .	186
7.4	Current data compared to Vasu's data on a linear scale . . . . .	187
7.5	Current data compared to Haylett's data on a linear scale . . . . .	188
7.6	Temperature drop from pure air vs. equivalence ratio . . . . .	191
7.7	Temperature drop from pure air vs. $T_5$ . . . . .	192
7.8	$n$ -Dodecane ignition delay comparison . . . . .	193
7.9	Diesel ignition delay comparison . . . . .	195
7.10	Current data compared to Wang et al. on linear scales . . . . .	196
7.11	Methyl oleate ignition delay comparison . . . . .	198
7.12	$x-t$ diagram of delayed drop removal . . . . .	201
7.13	Ignition delay data for all experiments . . . . .	202
8.1	Diesel ignition delay comparison . . . . .	208
8.2	Diesel ignition delay comparison showing error margins . . . . .	209
8.3	$x-t$ diagram of start of ignition including fuel acceleration . . . . .	211
A.1	Diesel combustion cycle . . . . .	214
A.2	Pre-chamber or indirect injection design . . . . .	215
A.3	Inline pump fuel injection system . . . . .	217
A.4	Common rail fuel injection system . . . . .	218
A.5	Unit injector fuel injection system . . . . .	219
A.6	Peak injection pressures . . . . .	220
B.1	System definition for apparent heat release rate calculation . . . . .	221

# List of Tables

2.1	Weight percent of fatty acids in various fat and oil feedstocks . . . .	9
2.2	Lower heating value for various fuels . . . . .	11
2.3	Example cetane numbers, measured with ASTM D613 . . . . .	23
2.4	Euro05 standards for compression ignition passenger vehicles . . . .	28
2.5	Damage estimates for emissions from diesel passenger cars . . . . .	29
2.6	Nitrogen oxide formation mechanism . . . . .	31
2.7	Shell model constants for <i>iso</i> -octane . . . . .	44
3.1	Sources and key for Fig. 3.7 . . . . .	79
5.1	Viscosity and derived cetane number . . . . .	106
5.2	Error estimates . . . . .	119
5.3	Specific emissions at approximately 50% load . . . . .	131
5.4	Specific emissions at approximately 93% load . . . . .	131
6.1	Required range of test conditions . . . . .	136
6.2	Shock strength and test conditions with air and helium drivers . . .	141
C.1	80% tallow/20% canola oil biodiesel . . . . .	226
C.2	100% tallow biodiesel . . . . .	228
C.3	50% tallow/50% palm oil biodiesel . . . . .	230
C.4	Methyl tallowate . . . . .	231
C.5	#2 diesel used in the shock tube . . . . .	232
D.1	Shock tube measurements of <i>n</i> -dodecane chemical ignition delay . .	235
D.2	Shock tube measurements of methyl oleate chemical ignition delay .	236
D.3	Shock tube measurements of #2 diesel chemical ignition delay . . .	237

# Abstract

Biodiesel is an alternative to diesel fuel that can reduce life-cycle greenhouse emissions. It is made from plant oils or waste animal fat. Changing an engine's fuel from #2 diesel to biodiesel does not require modifications to the engine, and has typically reduced emissions of particulate matter (PM) but increased nitrogen oxides ( $\text{NO}_x$ ). However, government regulations tightly limit exhaust pollutants, hence the increase is problematic.

In order to investigate the relationship between biodiesel fuel, ignition delay and emissions, experiments with a compression ignition, direct injection (CIDI) engine were performed. The emissions, ignition delays and apparent heat release rates from four locally produced biodiesel fuels and #2 diesel were measured. Emissions of  $\text{NO}_x$  were greater on average from the biodiesel fuels than the #2 diesel. Emissions of PM were not consistent, and measurements of ignition delay were the opposite of expectations. It was postulated that the fuel was undergoing atypical combustion, but this could not be confirmed with the limited data available from this investigation technique.

The engine experiments exemplified the need for alternative investigation techniques and numerical simulation of CIDI combustion was the leading choice. This technique was already well developed, however chemical ignition delay models for #2 diesel had received little validation and no data existed to generate a biodiesel chemical ignition delay model.

The novel drop method was conceived to measure the chemical ignition delay of heavy fuels at CIDI combustion relevant conditions and a shock tube was designed and built to use this method. It combusted fuel in a heterogeneous environment and minimised pre-experiment reactions. It was validated with *n*-dodecane, which indicated an assumed equivalence ratio at the ignition point was required. It then produced the first measurements of the chemical ignition delay of methyl oleate (a biodiesel surrogate) and #2 diesel at CIDI relevant conditions without pre-experimental reactions. Methyl oleate generated shorter chemical ignition delays than diesel and displayed NTC behaviour. The drop method shows strong potential for future measurements of the chemical ignition delay of many different heavy fuels.

# Acknowledgements

I used to believe that people can do anything they put their minds to. Now I realise what limits us is endurance, and without the support of every one of the following people I would have reached my limit a long time ago and never finished this thesis.

**The Playford Memorial Trust** are an organisation who have traditionally funded research into horticulture and aquaculture in South Australia. They kindly extended their areas of interest to include my research, and provided me with both a top up to my scholarship and a budget for my research. This budget financed and made possible the University of Adelaide Shock Tube.

**Elaine Boyd**, my caring wife. She has been a never ending source of encouragement, support and happiness, three things that I've certainly needed over the course of this thesis.

**Assoc. Prof. Con Doolan and Assoc. Prof. Colin Kestell**, my supervisors. Firstly, for taking me on as a student, then for being the perfect supervisors, and finally for always having my best interest at heart.

**My family**, and in particular my father. Dad has been my inspiration (or has been to blame, depending on your point of view) for my relentless desire to understand how everything works, no matter how simple or complicated. Watching him build instruments and computers in my formative years shaped my personality more than any other experience.

**Ken Boyd**, my grandfather. He pre-emptively bequeathed his estate to me near the start of my postgraduate work, stating that he wished to see what I did with it. Unfortunately he died before I could complete this thesis, but I think he would have been pleased that he helped support me during this work.

**Steven Kloeden** from the Mechanical Engineering Workshop, who has fixed many of my designs and gone beyond his job to assist me.

**Jason Peak** from the Chemical Engineering Workshop, who provided guidance and parts for the shock tube.

**Dr. Mike Riese**, whose off-the-cuff comment that I should put a drop of fuel on a wire in the shock tube developed into over half this thesis.

**Ian and all the crew at Bar 9**, my favourite coffee store. Not only did they introduce me to many great coffees, but the store was the perfect place to work, doubling my productivity. Near a third of this thesis was written there.

# Declaration of Originality

This work contains no material which has been accepted for the award of any other degree or diploma in any university or other tertiary institution to Marcus Boyd and, to the best of my knowledge and belief, contains no material previously published or written by another person, except where due reference has been made in the text.

I give consent to this copy of my thesis, when deposited in the University Library, being made available for loan and photocopying, subject to the provisions of the Copyright Act 1968. I also give permission for the digital version of my thesis to be made available on the web, via the University's digital research repository, the Library catalogue, the Australasian Digital Theses Program (ADTP) and also through web search engines.

*Signed*

---

Marcus Boyd

# Nomenclature

## Acronyms

AHRR	—	Apparent heat release rate, see Appendix B, page 221 for a definition
ARF	—	Australian Renewable Fuels
ATDC	—	After top dead centre
B30	—	A fuel comprised of 70% #2 diesel and 30% biodiesel
BP	—	British Petroleum
CI	—	Compression ignition
CIDI	—	Compression ignition, direct injection
CFD	—	Computational fluid dynamics
CN	—	Cetane number, see Sec. 2.2.3.1, page 23 for a definition
DI	—	Direct injection
EGR	—	Exhaust gas recirculation
FAME	—	Fatty acid methyl ester, see Sec. 2.1, page 7 for a definition
F–T diesel	—	Fischer–Tropsch diesel
GC/MS	—	Gas chromatography and mass spectrometry
GRI	—	Gas Research Institute
HCCI	—	Homogeneous charge compression ignition
HRR	—	Heat release rate
IDI	—	Indirect injection
JSR	—	Jet stirred reactor
KH/RT model	—	Kelvin–Helmholtz/Rayleigh–Taylor hybrid droplet breakup model
LHV	—	Lower heating value, see Sec. 2.1, page 10 for a definition
LLNL	—	Lawrence Livermore National Laboratory
NASA	—	National Aeronautics and Space Administration
NO <sub>x</sub>	—	Nitrogen oxides (NO & NO <sub>2</sub> )
NTC	—	Negative temperature coefficient
PAH	—	Poly–aromatic hydrocarbons
PM	—	Particulate matter
PRF	—	Primary reference fuel, a mixture of <i>iso</i> –octane and <i>n</i> –cetane
RCM	—	Rapid compression machine
RME	—	Rapeseed oil methyl ester, a biodiesel fuel

SAFF	—	Australian Farmers Federation
SOC	—	Start of combustion
SOI	—	Start of injection
TDC	—	Top dead centre
UoAST	—	University of Adelaide Shock Tube

## Symbols

$A$	—	Arrhenius pre-exponential factor
$A_{f_4}$	—	A key constant in the Shell model, for a definition see Sec. 2.4.2 on page 40
$a$	—	Speed of sound
$B$	—	An intermediate species in the Shell model
$B_0$	—	Breakup constant in the Kelvin–Helmholtz wave breakup theory
$C_b$	—	Breakup length constant in the Kelvin–Helmholtz wave breakup theory
$C_d$	—	Venturi meter discharge coefficient
$C_v$	—	Heat capacity at constant volume
$d$	—	Venturi meter throat diameter
$D_i$	—	Area at interface $i$ in L1d
$d_a$	—	Nozzle diameter in the Kelvin–Helmholtz wave breakup theory
$E$	—	Energy
$E_a$	—	Arrhenius activation energy
$EI_{NO_x}$	—	Nitrogen oxides emission index
$\phi$	—	Equivalence ratio, see Sec. 2.2.2, page 15 for a definition
$f_i$	—	Rate term for reaction $i$ in the Shell model
$F_{wall}$	—	Shear friction force at the wall in L1d
$F_{loss}$	—	Body-force due to losses from sudden changes in pipe diameter in L1d
$k$	—	Rate constant
$L_b$	—	Breakup length in the Kelvin–Helmholtz wave breakup theory
$m$	—	Mass
$M_s$	—	Incident shock Mach number
$MW_i$	—	Molecular weight of $i$
$n_i$	—	Number of moles of $i$
$P$	—	Pressure
$p_i$	—	Pressure in zone $i$ , see Fig. 2.23 on page 59 for a definition of shock tube zones
$Q$	—	An intermediate species in the Shell model, or the flow rate in the Venturi meter
$q$	—	Heat transfer

$Q_K$	—	Energy release in the Shell model
$Q_L$	—	Heat loss through the boundary walls in the Shell model
$R$	—	Universal gas constant
$\tilde{R}$	—	Molar gas constant
$\bar{R}$	—	All radicals in the Shell model
$r$	—	Radius
$r_c$	—	Radius of new droplets from the Kelvin–Helmholtz wave breakup theory
RH	—	The fuel in the Shell model
Re	—	Reynolds number
$T$	—	Temperature
$T_i$	—	Temperature in zone $i$ , see Fig. 2.23 on page 59 for a definition of shock tube zones
$t$	—	Time
Ta	—	Taylor number
$U_r$	—	Relative drop/gas velocity
$u$	—	Velocity
$V$	—	Volume
$v$	—	Rate of reaction
$v_i$	—	Stoichiometric number of substance $i$
$W_s$	—	Incident shock velocity
$W_r$	—	Reflected shock velocity
$We_g$	—	Gas Weber number
$Z$	—	Ohnesorge number
$\alpha$	—	Cut off ratio, see Sec. 5.3.2, page 126 for a definition
$\beta$	—	Venturi meter throat–to–pipe diameter ratio
$\gamma$	—	Ratio of specific heats
$\Delta_{KH}$	—	Wavelength of the fastest growing wave in the Kelvin–Helmholtz wave breakup theory
$\lambda$	—	Ratio of carbon monoxide to carbon dioxide in the Shell model
$\eta_{th}$	—	Thermal efficiency
$\rho$	—	Density
$\sigma$	—	Surface tension
$\tau_{id}$	—	Ignition delay
$\tau_{KH}$	—	Breakup time in the Kelvin–Helmholtz wave breakup theory
$\Omega_{KH}$	—	Growth rate of the fastest growing wave in the Kelvin–Helmholtz wave breakup theory